Chemiluminescence and Chemiluminescence Resonance Energy Transfer (CRET) Aptamer Sensors Using Catalytic Hemin/G-Quadruplexes

Xiaoqing Liu,† Ronit Freeman,† Eyal Golub, and Itamar Willner*

Institute of Chemistry, Center for Nanoscience and Nanotechnology, The Hebrew University of Jerusalem, Jerusalem 91904, Israel. †These authors contributed equally.

ABSTRACT The incorporation of hemin into the thrombin/G-quadruplex aptamer assembly or into the ATP/G-quadruplex nanostructure yields active DNAzymes that catalyze the generation of chemiluminescence. These catalytic processes enable the detection of thrombin and ATP with detection limits corresponding to 200 pM and 10 μM, respectively. The conjugation of the antithrombin or anti-ATP aptamers to CdSe/ZnS semiconductor quantum dots (QDs) allowed the detection of thrombin or ATP through the luminescence of the QDs that is powered by a chemiluminescence resonance energy-transfer (CRET) process stimulated by the hemin/G-quadruplex/thrombin complex or the hemin/G-quadruplex/ATP nanostructure, in the presence of luminol/H_2O_2. The advantages of applying the CRET process for the detection of thrombin or ATP, by the resulting hemin/G-quadruplex DNAzyme structures, are reflected by low background signals and the possibility to develop multiplexed aptasensor assays using different sized QDs.

KEYWORDS: chemiluminescence · resonance energy transfer · aptamer · sensor · quantum dot · thrombin · ATP

The development of aptasensors has attracted substantial research efforts in the past few years.[1−3] Electrical,[4,5] optical,[6−9] microgravimetric[10] and field-effect transistor[11] sensors, implementing the selective recognition properties of aptamers toward their substrates, were used to develop different sensing platforms. By the labeling of the aptamers with enzymes[12,13] or catalytic metal nanoparticles,[14,15] amplified aptasensors were fabricated. Also, catalytic nucleic acids were conjugated to aptamer sequences as amplifying labels.[16−18] Specifically, the hemin/G-quadruplex horseradish peroxidase (HRP)-mimicking DNAzyme[19,20] was used as an amplifying label to detect the formation of aptamer−substrate complexes.[21−23] The HRP-mimicking DNAzyme catalyzes the H_2O_2-mediated oxidation of $ABTS^{2-}$ to the colored product $ABTS^{\cdot -}$[19,20] or catalyzes the oxidation of luminol by H_2O_2 to yield chemiluminescence.[24] These functions of the DNAzyme were used to develop colorimetric or chemiluminescence aptasensors.[25−29] The unique size-controlled optical properties of semiconductor quantum dots (QDs) were extensively used for bioanalysis.[30−32] Different sized QDs were used as optical labels for the multiplexed analysis of DNA[33] or immuno-complexes.[34,35] Also, fluorescence resonance energy-transfer (FRET) process from QDs to dye acceptors was used to probe affinity complexes and enzymatic reactions.[36] Alternatively, QDs were used as energy acceptors from metal complexes[37] (*e.g.*, lanthanide complexes) or acceptors of energy generated by chemiluminescence[38,39] or bioluminescence.[40] These processes enable the use of a common energy source to excite different sized QDs for the development of multiplexed analysis assays. QDs were also used as luminescence[41−43] or photoelectrochemical[44] labels for the detection of aptamer−substrate complexes. Specifically, fluorescence resonance energy-transfer processes between QDs and dye acceptors were applied to follow the formation of supramolecular complexes between the target analyte and the aptamer subunits.[45] Recently, we reported on the use of the hemin/G-quadruplex HRP-mimicking DNAzyme, that is conjugated to semiconductor QDs, as a local, internal light source for promoting chemiluminescence resonance energy transfer (CRET) to semiconductor QDs.[38] This process was implemented for the detection of DNA and for the multiplexed analysis of different target DNAs, using different sized QDs. In fact, many of the aptamer sequences form G-quadruplexes (of variable number of G-quartet layers) upon their binding to the guest substrate (analyte). Thus, the incorporation of the hemin into

* Address correspondence to willnea@vms.huji.ac.il.

Received for review July 24, 2011 and accepted August 25, 2011.

Published online August 25, 2011
10.1021/nn202799d

such G-quadruplexes might lead to chemiluminescence labels, provided that the resulting hemin/G-quadruplexes are catalytically active. If, indeed, such hemin/G-quadruplexes reveal catalytic functions toward the generation of chemiluminescence, then the conjugation of these nanostructures to semiconductor QDs might lead to new CRET-based aptasensors. Here we report that the incorporation of hemin into the aptameric G-quadruplex–thrombin complex leads to a catalytic chemiluminescent DNAzyme structure. Also, we demonstrate for the first time that the binding of hemin to the aptameric G-quadruplex ATP complex results in a catalytically active DNAzyme. The conjugation of the nanostructures to CdSe/ZnS QDs yields new CRET-based sensors for thrombin and ATP.

RESULTS AND DISCUSSION

The antithrombin aptamer, (**1**), is widely used in different sensing platforms.[46–50] It is known to adopt a stable G-quadruplex structure upon its binding to thrombin.[51] The incorporation of hemin into the resulting G-quadruplex aptamer–thrombin complex yields an active HRP-mimicking DNAzyme that was used as a colorimetric sensor for thrombin by the H_2O_2 oxidation of $ABTS^{2-}$ to $ABTS^{\bullet -}$.[25] Figure 1A demonstrates the use of the hemin/G-quadruplex aptamer–thrombin complex for the generation of chemiluminescence in the presence of H_2O_2/luminol. Figure 1B shows the chemiluminescence spectra generated by the hemin/G-quadruplex aptamer–thrombin complex, in the presence of H_2O_2/luminol and different concentrations of thrombin. As the concentration of thrombin is elevated, the chemiluminescence is intensified, consistent with the higher content of the assembled DNAzyme. Control experiments reveal that the addition of a foreign protein, such as bovine serum albumin (BSA), shows no influence on the catalytic activity of the hemin–(**1**) complex. Figure 1C shows the derived calibration curve. The thrombin could be sensed with a detection limit of 200 pM. It should be noted that upon applying the colorimetric hemin/G-quadruplex aptamer-catalyzed oxidation of $ABTS^{2-}$ by H_2O_2 to analyze thrombin, the resulting detection limit corresponded to *ca.* 20 nM.[25] Thus, the chemiluminescent assay of thrombin reveals a *ca.* 100-fold enhanced sensitivity.

The chemiluminescence generated by the hemin/G-quadruplex aptamer–thrombin complex, at λ = 420 nm, is capable of exciting CdSe/ZnS QDs. Thus, the conjugation of the antithrombin aptamer to the QDs could yield, in the presence of thrombin, the chemiluminescent hemin/G-quadruplex aptamer–thrombin complex. The close proximity between the chemiluminescence light source and the QD could, then, lead to CRET to the QDs, a process that activates the luminescence of the QDs. Accordingly, the glutathione-modified CdSe/ZnS QDs were functionalized

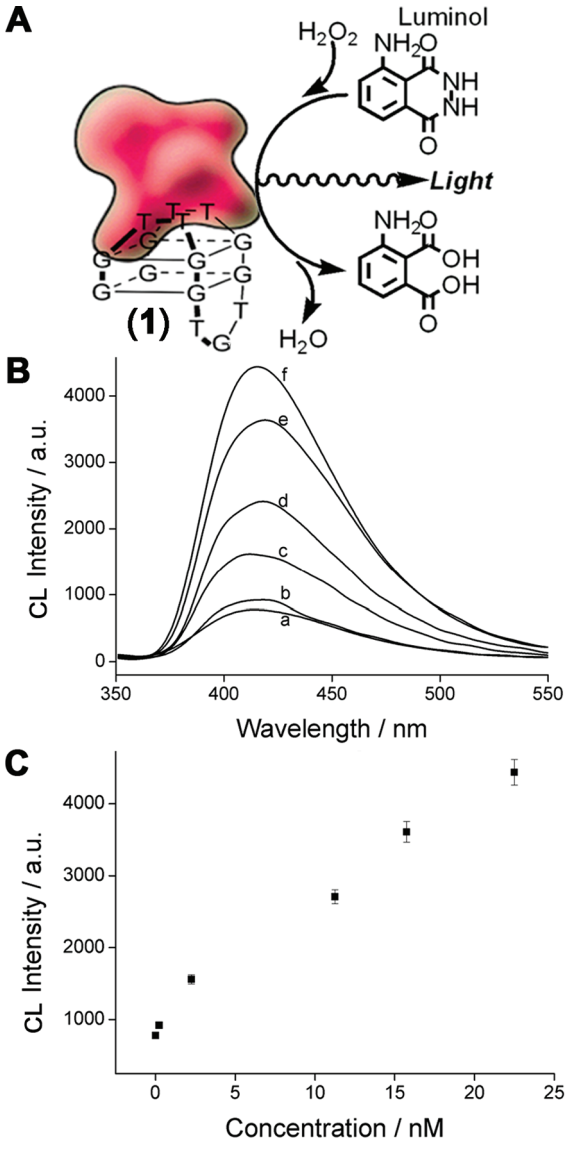

Figure 1. (A) Analysis of thrombin through the chemiluminescence of luminol generated by the hemin/thrombin aptamer complex. (B) Chemiluminescence intensities generated by the hemin–thrombin aptamer complex in the absence of thrombin, curve (a), and in the presence of variable concentrations of thrombin: (b) 0.225, (c) 2.25, (d) 11.25, (e) 15.75, and (f) 22.5 nM. (C) The derived calibration curve corresponding to the increase in the chemiluminescence signal at λ = 420 nm. Each data point is the average of *N* = 5 individual measurements. The error bars indicate the standard deviation.

with the antithrombin aptamer, (**2**), Figure 2A. The average coverage of the QDs by (**2**) corresponded to 10 aptamer units per QD (see Experimental Section). Figure 2B depicts the luminescence spectra of the system in the presence of hemin and different concentrations of thrombin. While, in the absence of thrombin, a low CRET signal and low chemiluminescence are observed (due to diffusional hemin), the addition of thrombin results in a high chemiluminescence and the respective CRET-stimulated luminescence of the QDs at λ = 615 nm. As the concentration of

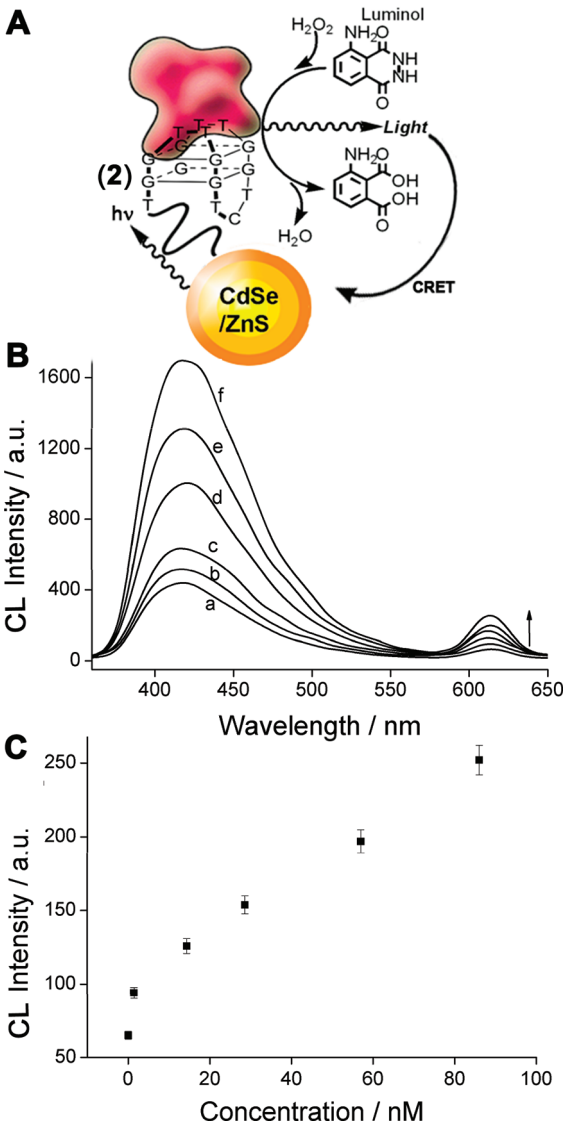

Figure 2. (A) Analysis of thrombin through the CRET from luminol, oxidized by the assembled hemin/G-quadruplex aptamer, to the QDs. (B) Luminescence spectrum corresponding to the chemiluminescence signal of the luminol and the CRET signal of the QDs in the absence of thrombin, curve (a), and in the presence of different concentrations of thrombin: (b) 1.43, (c) 14.3, (d) 28.6, (e) 57, and (f) 86 nM. (C) The derived calibration curve corresponding to the increase in the CRET signal at λ = 615 nm. Each data point is the average of N = 5 individual measurements. The error bars indicate the standard deviation.

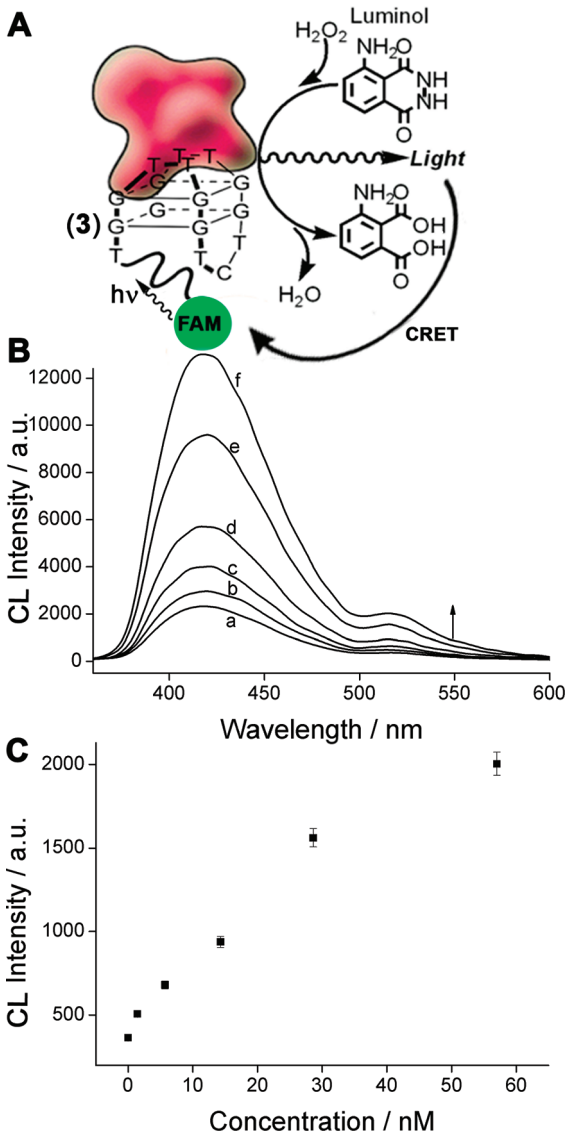

Figure 3. (A) Analysis of thrombin through the CRET from luminol, oxidized by the assembled hemin/G-quadruplex aptamer, to the fluorescein dye. (B) Luminescence spectrum corresponding to the chemiluminescence signal of the luminol and the CRET signal of the fluorescein in the absence of thrombin, curve (a), and in the presence of different concentrations of thrombin: (b) 1.43, (c) 5.7, (d) 14.3, (e) 28.6, and (f) 57 nM. (C) The derived calibration curve corresponding to the increase in the CRET signal at λ = 520 nm. Each data point is the average of N = 5 individual measurements. The error bars indicate the standard deviation.

thrombin is elevated, the CRET signals are intensified, consistent with the higher content of DNAzyme units generated upon the increase of the concentration of thrombin. Figure 2C depicts the resulting calibration curve using the CRET signal as the readout stimulus. Thrombin is sensed with a detection limit that corresponds to 1.4 nM. The CRET efficiency, E, was calculated following eq 1, where I(A) and I(D) correspond to the integral areas of the acceptor and donor emissions, respectively, and QY(A) corresponds to the luminescence quantum yield of the acceptor. Accordingly, knowing the CRET efficiency, 20%, and the geometrical separation between the QDs and the G-quadruplex, we estimated the Förster radius to be *ca.* 2.7 nm.

$$E = [I(A)/QY(A)]/[I(D) + I(A)/QY(A)] \quad (1)$$

The CRET process, using the hemin/G-quadruplex aptamer−thrombin complex, is not limited to the QDs. Upon the substitution of the QDs with the acceptor dye, fluorescein, using the nucleic acid, (**3**), a similar CRET process was observed, as demonstrated in Figure 3. The CRET efficiency was calculated using eq 1, to be

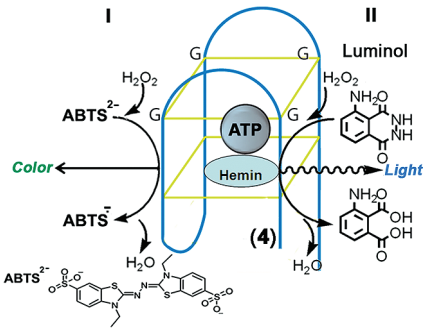

Figure 4. Colorimetric (I) and chemiluminescent (II) analysis of ATP by the formation of hemin/ATP-G-quadruplex structure.

12%, and the Förster radius was estimated to be *ca.* 1.8 nm.

Other aptamers, besides the thrombin-binding aptamer, which consist of G-rich DNA sequences, can adopt a G-quadruplex conformation. Therefore, they are anticipated to incorporate hemin and form catalytically active structures that could, then, serve as biocatalytic amplifying labels upon the formation of the aptamer–substrate complexes. One of the G-quadruplex-forming aptamers is the aptamer for ATP, (**4**), that generates a G-quadruplex nanostructure that consists of two stacked G-quartets.[52] Treatment of the resulting ATP-G-quadruplex structure with hemin results in the hemin/G-quadruplex that acts as a HRP-mimicking DNAzyme. This results in the catalytic activity toward the H_2O_2 oxidation of $ABTS^{2-}$ to $ABTS^{\cdot-}$ or the generation of chemiluminescence in the presence of H_2O_2/luminol, as depicted in Figure 4. This process provides the basis for the analysis of ATP. Figure 5A shows the time-dependent formation of $ABTS^{\cdot-}$ in the presence of different concentrations of ATP. As the concentration of ATP increases, the rate of $ABTS^{\cdot-}$ formation is intensified, consistent with the higher content of the hemin/G-quadruplex-ATP DNAzyme. A control experiment reveals that in the absence of the aptamer sequence, only residual activity of the hemin is observed. Figure 5B presents the derived calibration curve that shows the absorbance of $ABTS^{\cdot-}$ after a fixed time interval of activation of the DNAzyme, in the presence of different concentrations of ATP. The catalytic hemin/G-quadruplex ATP aptamer enabled, also, the generation of chemiluminescence, in the presence of H_2O_2 and luminol. Figure 6A shows the chemiluminescence spectra generated by the hemin/G-quadruplex ATP aptamer complex, in the presence of H_2O_2/luminol and different concentrations of ATP. As the concentration of ATP is elevated, the chemiluminescence is intensified, consistent with the higher content of the assembled DNAzyme. Figure 6B shows the derived calibration curve. It should be noted that for both the colorimetric and chemiluminescent approaches the sensing of ATP is specific, and the interaction of (**4**) in the presence of adenosine

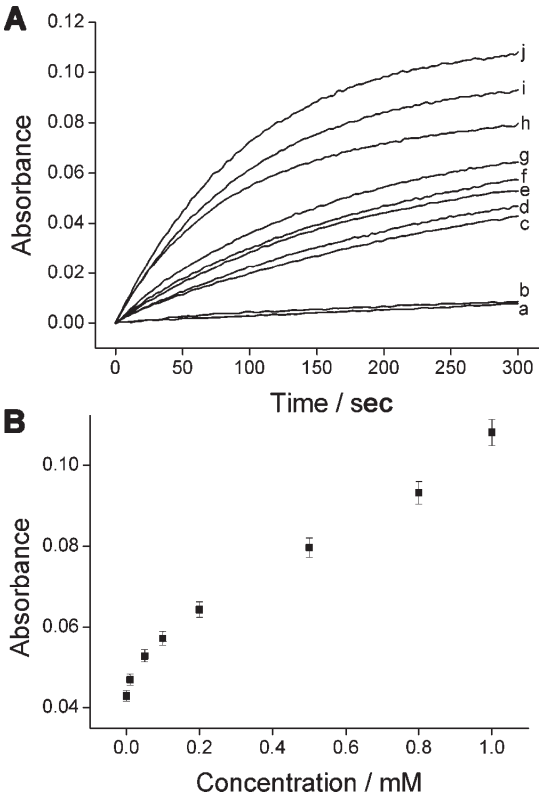

Figure 5. (A) Time-dependent absorbance changes of $ABTS^{\cdot-}$ by 0.5 μM hemin (a) in the absence of ATP and (b) in the presence of 1000 μM ATP. (c–j) Time-dependent absorbance changes of $ABTS^{\cdot-}$ by 0.5 μM hemin and 0.25 μM ATP aptamer upon analyzing different concentrations of ATP: (c) 0, (d) 10, (e) 50, (f) 100, (g) 200, (h) 500, (i) 800, and (j) 1000 μM. (B) Calibration curve corresponding to the analysis of different concentrations of ATP. Each data point is the average of $N = 5$ individual measurements. The error bars indicate the standard deviation.

monophosphate (AMP) or adenosine diphosphate (ADP) yielded low signals. Furthermore, guanosine 5′-triphosphate (GTP), cytidine 5′-triphosphate (CTP), and uridine 5′-triphosphate (UTP) demonstrated no affinity for the aptamer, leading to the background signal of the system in the absence of any analyte. Also, the influence of ATP on the catalytic activity of a G-quadruplex DNAzyme was examined using a foreign G-quadruplex, (**5**), that lacks affinity for ATP. The results show that the generated chemiluminescence was stable and was not affected by the added ATP. These results indicate that ATP, indeed, binds to the aptamer (**4**), and that it stimulates its catalytic activity.

Since the hemin/anti-ATP G-quadruplex aptamer reveals catalytic functions toward the generation of chemiluminescence, the conjugation of the aptamer to semiconductor QDs will trigger-on the chemiluminescence resonance energy-transfer process and the luminescence of the QDs, thus enabling the use of the conjugates as luminescent probes for the analysis of aptamer–substrate complexes. Accordingly, glutathione-modified QDs were functionalized with the nucleic acid, (**6**), that includes the aptamer sequence

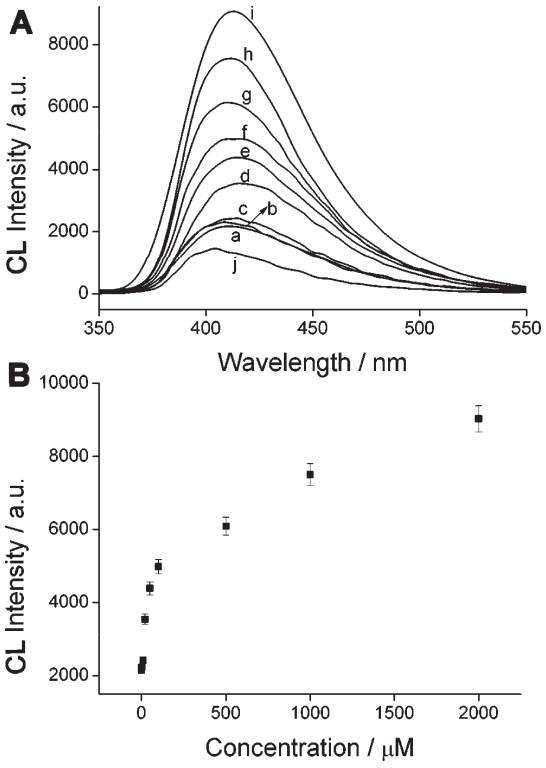

Figure 6. (A) Chemiluminescence intensities generated by the hemin/ATP aptamer in the absence of ATP, curve (a), and in the presence of variable concentrations of ATP: (b) 1, (c) 10, (d) 20, (e) 50, (f), 100, (g) 500, (h) 1000, and (i) 2000 μM. (j) Chemiluminescence intensity generated by 0.5 μM hemin in the presence of 100 μM ATP, but in the absence of the aptamer. (B) The derived calibration curve corresponding to the increase in the chemiluminescence signal at λ = 415 nm. Each data point is the average of N = 5 individual measurements. The error bars indicate the standard deviation.

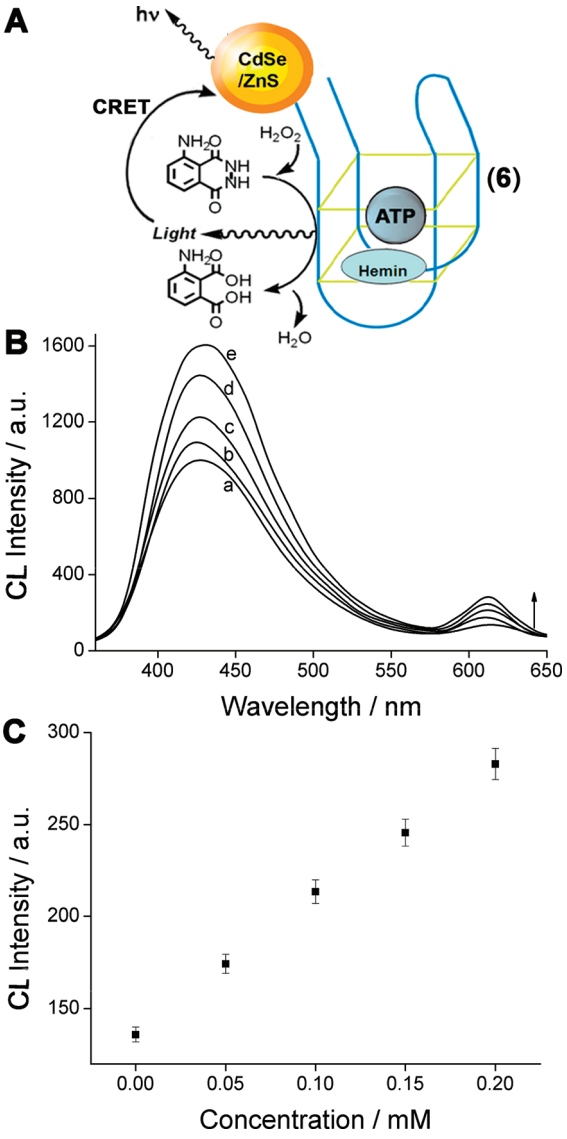

Figure 7. (A) Analysis of ATP through the CRET from luminol, oxidized by the assembled hemin/ATP aptamer, to the QDs. (B) Luminescence spectrum corresponding to the chemiluminescence signal of the luminol and the CRET signal of the QDs in the absence of ATP, curve (a), and in the presence of different concentrations of ATP: (b) 0.05, (c) 0.1, (d) 0.15, and (e) 0.2 mM. (C) The derived calibration curve corresponding to the increase in the CRET signal of the QDs at λ = 612 nm. Each data point is the average of N = 5 individual measurements. The error bars indicate the standard deviation.

for ATP, tethered to the QDs with an oligo-T spacer, Figure 7A (average loading of *ca*. 10 units per QD, see Experimental Section). Figure 7B shows the luminescence spectra of the system in the presence of H_2O_2/luminol and variable concentrations of ATP. In addition to the chemiluminescence generated by the DNAzyme-catalyzed oxidation of luminol by H_2O_2, the characteristic luminescence of the QDs at λ = 615 nm is detected, implying that a CRET process occurs in the system. As the concentration of ATP increases, the CRET signal is intensified (Figure 7C), consistent with the higher content of the chemiluminescence-generating DNAzyme that results in an enhanced intensity of the chemiluminescent light source. From the resulting luminescence spectra and using eq 1, we determined the CRET efficiency to be 19% and estimated the Förster distance to be *ca*. 4.6 nm. Control experiments confirmed that the CRET process occurs only in the presence of ATP. No CRET change was observed upon the linking of a foreign nonaptameric nucleic acid (**7**) to the QDs, in the presence of hemin and different concentrations of ATP (see Figure S1, Supporting Information). These results imply that the catalytic hemin/G-quadruplex is formed only in the presence of the specific substrate and that the intimate distance between the catalytic DNAzyme, and the QDs is essential to stimulate the CRET process. One should note, however, that since the hemin/G-quadruplex also quenches the luminescence of the QDs *via* electron transfer,[43] modifying the QDs with the aptamer without using any spacer, nucleic acid (**8**), results in decreased chemiluminescene and CRET signals when interacting the (**8**)-modified QDs with increasing concentrations of ATP. It should be noted that the CRET chemiluminescence values for the thrombin system, Figure 2C, and ATP system, Figure 7C are within the

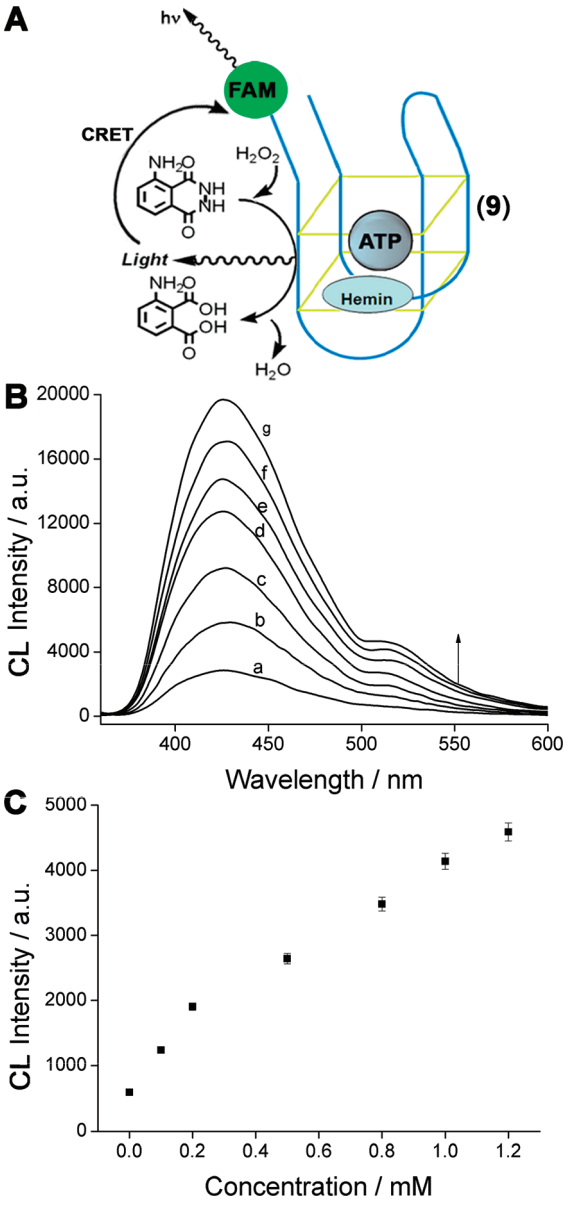

Figure 8. (A) Analysis of ATP through the CRET from luminol, oxidized by the assembled hemin/ATP aptamer, to the fluorescein dye. (B) Luminescence spectrum corresponding to the chemiluminescence signal of the luminol and the CRET signal of fluorescein in the absence of ATP, curve (a), and in the presence of different concentrations of ATP: (b) 0.1, (c) 0.2, (d) 0.5, (e) 0.8, (f) 1, and (g) 1.2 mM. (C) The derived calibration curve corresponding to the increase in the CRET signal at $\lambda = 520$ nm. Each data point is the average of $N = 5$ individual measurements. The error bars indicate the standard deviation.

same magnitude but are observed in different ranges of concentrations of the respective substrates. This is consistent with the higher affinity of thrombin to its aptamer ($K_d \approx 25$ nM)[51] as compared to ATP to its aptamer ($K_d \approx 6$ μM).[52] In fact, analyzing the calibration curves in Figures 2C and 7C according to a Langmuir-type complexation yields $K_d \approx 3$ nM for thrombin and $K_d \approx 13$ μM for ATP to the respective aptamers, consistent with the literature data.

The CRET process between the hemin/G-quadruplex-aptamer-ATP complexes is not limited to the QDs, and upon the substitution of the QDs with the fluorescein dye as an acceptor, a similar CRET process was observed, Figure 8. In the presence of nucleic acid, (**9**), and using eq 1, the CRET efficiency is estimated to be 16%, and the Förster radius is *ca.* 2.8 nm. Control experiments show that the generation of the CRET signal is specific to ATP, and no CRET signal was observed in the presence of AMP, ADP, CTP, GTP, and UTP (see Supporting Information, Figure S2).

It should be noted that the CRET process to the dye molecules, in both thrombin and ATP systems, requires a higher concentration of the aptamer G-quadruplex, then the concentration used in the QDs systems, in order to trigger on the fluorescence of the dye. This difference originates from the fact that each QD is decorated with *ca.* 10 aptamer units, resulting in a more efficient CRET process. However, each dye is linked to only one aptamer, and therefore, higher concentration is needed in order to achieve a similar CRET efficiency.

CONCLUSIONS

The present study has demonstrated that different G-quadruplex aptamers can bind hemin and turn into catalytically active DNAzymes that generate chemiluminescence in the presence of H_2O_2/luminol. Specifically, we have demonstrated for the first time, that the ATP G-quadruplex aptamer can bind hemin to form a complex that reveals DNAzyme-like catalytic activity. The conjugation of the aptameric-G-quadruplexes to QDs enabled the use of the chemiluminescence process as an internal light source for stimulating the CRET process. The advantages involved with the application of the CRET process as a readout signal include: (i) The close proximity between the chemiluminescent probe and the QDs is essential to enable the CRET process. This eliminates background signals, *e.g.*, of diffusional hemin. (ii) The possibility to excite different sized QDs with the chemiluminescence signal enables the generation of different luminescence spectra controlled by the different QDs, thus allowing the construction of multiplexed aptamer-based sensors.

EXPERIMENTAL SECTION

Materials and Reagents. Hops yellow core shell EviDots, CdSe/ZnS quantum dots in toluene, were purchased from Evident Technologies. *N*-[*e*-maleimidocaproyloxy]succinimide ester (EMCS) and bis[sulfosuccinimidyl] suberate (BS_3) were purchased from Pierce Biotechnologies. NaCl, KCl, $NaNO_3$, KNO_3, trizma hydrochloride, trizma base, 4-(2-hydroxyethyl)piperazine-1-ethanesulfonic acid sodium salt (HEPES), 2,2′-azinobis(3-ethylbenzothiazoline)-6-sulfonate ($ABTS^{2-}$), luminol, adenosine 5′-triphosphate (ATP), adenosine 5′-diphosphate sodium salt (ADP), adenosine 5′-monophosphate disodium salt (AMP), guanosine 5′-triphosphate (GTP),

cytidine 5′-triphosphate (CTP), uridine 5′-triphosphate (UTP), bovine serum albumin (BSA), and thrombin were purchased from Sigma-Aldrich. Ultrapure water from a NANOpure Diamond (Barnstead Int., Dubuque, IA) source was used throughout the experiments.

Oligonucleotides were custom-ordered from Sigma Life Science (U.K.). All oligonucleotides were HPLC-purified and freeze-dried by the supplier. The oligonucleotides were used as provided and diluted in pH 7.5, 10 mM of phosphate buffer solution to give stock solutions of 100 μM.

The sequences of the oligomers are as follows:

(1) 5′-GGTTGGTGTGGTTGG-3′
(2) 5′-$H_2N(CH_2)_6$TTGGTTGGTGTGGTTGG-3′
(3) 5′-FAM$(CH_2)_6$TTTGGTTGGTGTGGTTGG-3′
(4) 5′-ACCTGGGGGAGTATTGCGGAGGAAGGT-3′
(5) 5′-GGGTAGGGCGGGTTGGG-3′
(6) 5′-$H_2N(CH_2)_{12}$TTTTTTTTTTTACCTGGGGGAGTATTGCGGAGGAAGG-3′
(7) 5′-HS$(CH_2)_6$AAAATACCTGGGGGAGTATATAGGG-3′
(8) 5′-$H_2N(CH_2)_6$ACCTGGGGGAGTATTGCGGAGGAAGG-3′
(9) 5′-FAM$(CH_2)_6$TTTTTTTTTTACCTGGGGGAGTATTGCGGAGGAAGG-3′

Preparation of GSH-Capped QDs and Nucleic Acid-Modified CdSe/ZnS QDs and the Calculation of the Loading of the Nucleic Acids on the QDs. The preparation of the GSH-QDs, the nucleic acid-modified QDs and the determination of DNA/QDs ratio followed the previously reported methods.[38]

Analysis of ATP and Thrombin by Colorimetric and Chemiluminescence Methods. The ATP aptamer or the thrombin aptamer were diluted in Tris buffer (12.5 mM of Tris, 150 mM of NaCl, 25 mM of KCl, pH 7.2) or HEPES buffer (25 mM of HEPES, 20 mM of KNO_3, 200 mM of $NaNO_3$, pH 7.4), respectively, heated to 90 °C for 5 min and slowly cooled down to room temperature. Different concentrations of ATP or thrombin were added to the annealed aptamer. The system was allowed to incubate for 2 h at room temperature. Then, hemin was added and incubated for 1 h at room temperature to form the respective hemin/G-quadruplex structures.

The colorimetric assay for analyzing ATP was performed in a solution containing 0.25 μM of ATP aptamer, 0.5 μM of hemin, 2 mM of $ABTS^{2-}$, and 5 mM of H_2O_2. Briefly, 160 μL of Tris buffer (pH 7.2), 20 μL of DNAzyme solution, 10 μL of $ABTS^{2-}$ (40 mM), and 10 μL of H_2O_2 (100 mM) were added to a cuvette. Absorbance changes were recorded at a fixed time interval of 5 min. The rate of the peroxidase-mimicking reaction was monitored at λ = 414 nm.

The chemiluminescence assays for analyzing ATP or thrombin were performed in a cuvette that included 0.25 μM of ATP aptamer or thrombin aptamer, 0.5 μM of hemin, 0.5 mM of luminol, and 30 mM of H_2O_2. Briefly, 50 μL of DNAzyme solution, 200 μL of Tris buffer or HEPES buffer (pH 9), and 50 μL of 5 mM luminol solution were added to a cuvette. Then, 200 μL of H_2O_2 (75 mM) stock solution was quickly added. The light emission intensity was measured immediately.

Analysis of ATP and Thrombin by the DNAzyme-Modified QDs/Dye Using CRET as the Readout Signal. The ATP aptamer modified with QDs or fluorescein was incubated with different concentrations of ATP or thrombin for 2 h, followed by the addition of hemin for an additional incubation of 1 h. The CRET assay for analyzing ATP was performed in a cuvette that included the modified QDs (50 nM) and hemin (0.25 μM) or the fluorescein-modified aptamer (2 μM) and hemin (1 μM). Measurements were performed in Tris buffer (12.5 mM of Tris, 150 mM of NaCl, 25 mM of KCl, pH 9) with 0.5 mM of luminol and 3.75 mM of H_2O_2.

The CRET assay for analyzing thrombin was performed in a cuvette that included the modified QDs (50 nM) or the fluorescein-modified aptamer (5 μM), and 1 μM of hemin, 0.5 mM of luminol, and 3.75 mM of H_2O_2. Measurements were performed in HEPES buffer (25 mM of HEPES, 5 mM of KNO_3, 50 mM of $NaNO_3$, pH 9) after addition of luminol and H_2O_2. The light emission intensities were measured immediately.

Determination of the Detection limit. The detection limit corresponds to the lowest detectable concentration that can be distinguished from the background signal by 10% in N = 5 experiments.

Optical Instrumentation. Absorbance measurements were performed using a Shimadzu UV-2401PC UV–vis spectrophotometer. Light emission experiments were carried out using a photoncounting spectrometer (Edinburgh Instruments, FLS 920) equipped with a cooled photomultiplier detection system connected to a computer (F900 v.6.3 software, Edinburgh Instruments).

Acknowledgment. The research is supported by the EU FP7 project NANOGNOSTICS.

Supporting Information Available: Control experiments for the CRET system analyzing ATP. Modification of the QDs with a foreign, nonaptameric nucleic acid, and examining the specificity of the CRET to dye system in the presence of different phosphonucleotides. This material is available free of charge *via* the Internet at http://pubs.acs.org.

REFERENCES AND NOTES

1. Iliuk, A. B.; Hu, L.; Tao, W. A. Aptamer in Bioanalytical Applications. *Anal. Chem.* **2011**, *83*, 4440–4452.
2. Keefe, A. D.; Pai, S.; Ellington, A. Aptamers As therapeutics. *Nat. Rev. Drug Discovery* **2010**, *9*, 537–550.
3. Fang, X.; Tan, W. Aptamers Generated from Cell-SELEX for Molecular Medicine: A Chemical Biology Approach. *Acc. Chem. Res.* **2010**, *43*, 48–57.
4. Wang, J.; Liu, G.; Merkoci, A. Electrochemical Coding Technology for Simultaneous Detection of Multiple DNA Targets. *J. Am. Chem. Soc.* **2003**, *125*, 3214–3215.
5. Swensen, J. S.; Xiao, Y.; Ferguson, B. S.; Lubin, A. A.; Lai, R. Y.; Heeger, A. J.; Plaxco, K. W.; Soh, H. T. Continuous, Real-Time Monitoring of Cocaine in Undiluted Blood Serum via a Microfluidic, Electrochemical Aptamer-Based Sensor. *J. Am. Chem. Soc.* **2009**, *131*, 4262–4266.
6. Wang, H.; Yang, R.; Yang, L.; Tan, W. Nucleic Acid Conjugated Nanomaterials for Enhanced Molecular Recognition. *ACS Nano* **2009**, *3*, 2451–2460.
7. Liu, J.; Cao, Z.; Lu, Y. Functional Nucleic Acid Sensors. *Chem. Rev.* **2009**, *109*, 1948–1998.
8. Zheng, D.; Seferos, D. S.; Giljohann, D. A.; Patel, P. C.; Mirkin, C. A. Aptamer Nano-flares for Molecular Detection in Living Cells. *Nano Lett.* **2009**, *9*, 3258–3261.
9. Tang, Z.; Mallikaratchy, P.; Yang, R.; Kim, Y.; Zhu, Z.; Wang, H.; Tan, W. Aptamer Switch Probe Based on Intramolecular Displacement. *J. Am. Chem. Soc.* **2008**, *130*, 11268–11269.
10. Liss, M.; Petersen, B.; Wolf, H.; Prohaska, E. An Aptamer-Based Quartz Crystal Protein Biosensor. *Anal. Chem.* **2002**, *74*, 4488–4495.
11. Sharon, E.; Freeman, R.; Tel-Vered, R.; Willner, I. Impedimetric or Ion-Sensitive Field-Effect Transistor (ISFET) Aptasensors Based on the Self-Assembly of Au Nanoparticle-Functionalized Supramolecular Aptamer Nanostructures. *Electroanalysis* **2009**, *21*, 1291–1296.
12. Li, Y.; Lee, H. J.; Corn, R. M. Detection of Protein Biomarkers Using RNA Aptamer Microarrays and Enzymatically Amplified Surface Plasmon Resonance Imaging. *Anal. Chem.* **2007**, *79*, 1082–1088.
13. Baldrich, E.; Acero, J. L.; Reekmans, G.; Laureyn, W.; O'Sullivan, C. K. Displacement Enzyme Linked Aptamer Assay. *Anal. Chem.* **2005**, *77*, 4774–4784.
14. Levy, M.; Cater, S. F.; Ellington, A. D. Quantum-Dot Aptamer Beacons for the Detection of Proteins. *ChemBioChem* **2005**, *6*, 2163–2166.
15. Polsky, R.; Gill, R.; Kaganovsky, L.; Willner, I. Nucleic Acid-Functionalized Pt Nanoparticles: Catalytic Labels for the Amplified Electrochemical Detection of Biomolecules. *Anal. Chem.* **2006**, *78*, 2268–2271.
16. Höbartner, C.; Silverman, S. K. Recent Advances in DNA Catalysis. *Biopolymers* **2007**, *87*, 279–292.
17. Willner, I.; Shlyahovsky, B.; Zayats, M.; Willner, B. DNAzymes for Sensing, Nanobiotechnology and Logic Gate Applications. *Chem. Soc. Rev.* **2008**, *37*, 1153–1165.

18. Zhang, X.-B.; Kong, R.-M.; Lu, Y. Metal Ion Sensors Based on DNAzymes and Related DNA Molecules. *Annu. Rev. Anal. Chem.* **2011**, *4*, 105–128.
19. Travascio, P.; Li, Y.; Sen, D. DNA-Enhanced Peroxidase Activity of a DNA Aptamer-Hemin Complex. *Chem. Biol.* **1998**, *5*, 505–517.
20. Travascio, P.; Bennet, A. J.; Wang, D. Y.; Sen, D. A Ribozyme and a Catalytic DNA with Peroxidase Activity: Active Sites Versus Cofactor-Binding Sites. *Chem. Biol.* **1999**, *6*, 779–787.
21. Teller, C.; Shimron, S.; Willner, I. Aptamer-DNAzyme Hairpins for Amplified Biosensing. *Anal. Chem.* **2009**, *81*, 9114–9119.
22. Pelossof, G.; Tel-Vered, R.; Elbaz, J.; Willner, I. Amplified Biosensing Using the Horseradish Peroxidase-Mimicking DNAzyme as an Electrocatalyst. *Anal. Chem.* **2010**, *82*, 4396–4402.
23. Pelossof, G.; Tel-Vered, R.; Liu, X. Q.; Willner, I. Amplified Surface Plasmon Resonance-Based DNA Biosensors, Aptasensors, and Hg^{2+} Sensors Using Hemin/G-Quadruplexes and Au Nanoparticles. *Chem.—Eur. J.* **2011**, *17*, 8904–8912.
24. Xiao, Y.; Pavlov, V.; Gill, R.; Bourenko, T.; Willner, I. Lighting Up Biochemiluminescence by the Surface Self-Assembly of DNA-Hemin Complexes. *ChemBioChem* **2004**, *5*, 374–379.
25. Li, T.; Wang, E.; Dong, S. G-quadruplex-Based DNAzyme for Facile Colorimetric Detection of Thrombin. *Chem. Commun.* **2008**, 3654–3656.
26. Li, T.; Wang, E.; Dong, S. Chemiluminescence Thrombin Aptasensor Using High-Activity DNAzyme As Catalytic Label. *Chem. Commun.* **2008**, 5520–5522.
27. Bi, S.; Li, L.; Zhang, S. Triggered Polycatenated DNA Scaffolds for DNA Sensors and Aptasensors by a Combination of Rolling Circle Amplification and DNAzyme Amplification. *Anal. Chem.* **2010**, *82*, 9447–9454.
28. Elbaz, J.; Moshe, M.; Shlyahovsky, B.; Willner, I. Cooperative Multicomponent Self-Assembly of Nucleic Acid Structures for the Activation of DNAzyme Cascades: A Paradigm for DNA Sensors and Aptasensors. *Chem.—Eur. J.* **2009**, *15*, 3411–3418.
29. Li, D.; Shlyahovsky, B.; Elbaz, J.; Willner, I. Amplified Analysis of Low-Molecular-Weight Substrates or Proteins by the Self-Assembly of DNAzyme-Aptamer Conjugates. *J. Am. Chem. Soc.* **2007**, *129*, 5804–5805.
30. Medintz, I. L.; Uyeda, H. T.; Goldman, E. R.; Mattoussi, H. Quantum Dot Bioconjugates for Imaging, Labelling and Sensing. *Nat. Mater.* **2005**, *4*, 435–446.
31. Freeman, R.; Xu, J.-P.; Willner, I. Semiconductor Quantum Dots (QDs) for Analytical and Bioanalytical Applications. In *Nanoparticles: From Theory to Application*; Schmid, G., Ed.; Wiley-VCH: Weinheim, Germany, 2010; Chapter 6, pp 455–511.
32. Resch-Genger, U.; Grabolle, M.; Cavaliere-Jaricot, S.; Nitschke, R.; Nann, T. Quantum Dots Versus Organic Dyes as Fluorescent Labels. *Nat. Methods* **2008**, *5*, 763–775.
33. Gao, Y.; Stanford, W. L.; Chan, W. C. W. Quantum-Dot-Encoded Microbeads for Multiplexed Genetic Detection of Non-amplified DNA Samples. *Small* **2011**, *7*, 137–146.
34. Liu, J.; Lau, S. K.; Varma, V. A.; Kairdolf, B. A.; Nie, S. Multiplexed Detection and Characterization of Rare Tumor Cells in Hodgkin's Lymphoma with Multicolor Quantum Dots. *Anal. Chem.* **2010**, *82*, 6237–6243.
35. Jennings, T. L.; Becker-Catania, S. G.; Triulzi, R. C.; Tao, G.; Scott, B.; Sapsford, K. E.; Spindel, S.; Oh, E.; Jain, V.; Delehanty, J. B.; et al. Reactive Semiconductor Nanocrystals for Chemoselective Biolabeling and Multiplexed Analysis. *ACS Nano* **2011**, *5*, 5579–5593.
36. Medintz, I. L.; Clapp, A. R.; Brunel, F. M.; Tiefenbrunn, T.; Uyeda, H. T.; Chang, E. L.; Deschamps, J. R.; Dawson, P. E.; Mattoussi, H. Proteolytic Activity Monitored by Fluorescence Resonance Energy Transfer Through Quantum-Dot–Peptide Conjugates. *Nat. Mater.* **2006**, *5*, 581–589.
37. Geißler, D.; Charbonnière, L. J.; Ziessel, R. F.; Butlin, N. G.; Löhmannsröben, H. G.; Hildebrandt, N. Quantum Dot Biosensors for Ultrasensitive Multiplexed Diagnostics. *Angew. Chem., Int. Ed.* **2010**, *49*, 1396–1401.
38. Freeman, R.; Liu, X. Q.; Willner, I. Chemiluminescent and Chemiluminescence Resonance Energy Transfer (CRET) Detection of DNA, Metal Ions, and Aptamer_Substrate Complexes Using Hemin/G-Quadruplexes and CdSe/ZnS Quantum Dots. *J. Am. Chem. Soc.* **2011**, *133*, 11597–11604.
39. Huang, X.; Li, L.; Qian, H.; Dong, C.; Ren, J. A Resonance Energy Transfer between Chemiluminescence Donors and CdTe Quantum Dots Acceptors (CRET). *Angew. Chem., Int. Ed.* **2006**, *45*, 5140–5143.
40. So, M. K.; Xu, C.; Loening, A. M.; Gambhir, S. S.; Rao, J. Self-Illuminating Quantum Dot Conjugates for *In Vivo* Imaging. *Nat. Biotechnol.* **2006**, *24*, 339–343.
41. Choi, J. H.; Chen, K. H.; Strano, M. S. Aptamer-Capped Nanocrystal Quantum Dots: A New Method for Label-Free Protein Detection. *J. Am. Chem. Soc.* **2006**, *128*, 15584–15585.
42. Bagalkot, V.; Zhang, L.; Levy-Nissenbaum, E.; Jon, S.; Kantoff, P. W.; Langer, R.; Farokhzad, O. C. Quantum Dot-Aptamer Conjugates for Synchronous Cancer Imaging, Therapy, and Sensing of Drug Delivery Based on Bi-Fluorescence Resonance Energy Transfer. *Nano Lett.* **2007**, *7*, 3065–3070.
43. Sharon, E.; Freeman, R.; Willner, I. CdSe/ZnS Quantum Dots-G-Quadruplex/Hemin Hybrids as Optical DNA Sensors and Aptasensors. *Anal. Chem.* **2010**, *82*, 7073–7077.
44. Golub, E.; Pelossof, G.; Freeman, R.; Zhang, H.; Willner, I. Electrochemical, Photoelectrochemical, and Surface Plasmon Resonance Detection of Cocaine Using Supramolecular Aptamer Complexes and Metallic or Semiconductor Nanoparticles. *Anal. Chem.* **2009**, *81*, 9291–9298.
45. Freeman, R.; Li, Y.; Tel-Vered, R.; Sharon, E.; Elbaz, J.; Willner, I. Self-Assembly of Supramolecular Aptamer Structures for Optical or Electrochemical Sensing. *Analyst* **2009**, *134*, 653–656.
46. Pavlov, V.; Xiao, Y.; Shlyahovsky, B.; Willner, I. Aptamer-Functionalized Au Nanoparticles for the Amplified Optical Detection of Thrombin. *J. Am. Chem. Soc.* **2004**, *126*, 11768–11769.
47. Xiao, Y.; Lubin, A. A.; Heeger, A. J.; Plaxco, K. W. Label-Free Electronic Detection of Thrombin in Blood Serum by Using an Aptamer-Based Sensor. *Angew. Chem., Int. Ed.* **2005**, *44*, 5456–5459.
48. Gill, R.; Polsky, R.; Willner, I. Pt Nanoparticles Functionalized with Nucleic Acid Act as Catalytic Labels for the Chemiluminescent Detection of DNA and Proteins. *Small* **2006**, *2*, 1037–1041.
49. Lin, C.; Katilius, E.; Liu, Y.; Zhang, J.; Yan, H. Self-Assembled Signaling Aptamer DNA Arrays for Protein Detection. *Angew. Chem., Int. Ed.* **2006**, *45*, 5296–5301.
50. Huang, Y. C.; Ge, B.; Sen, D.; Yu, H. Z. Immobilized DNA Switches as Electronic Sensors for Picomolar Detection of Plasma Proteins. *J. Am. Chem. Soc.* **2008**, *130*, 8023–8029.
51. Bock, L. C.; Griffin, L. C.; Latham, J. A.; Vermaas, E. H.; Toole, J. J. Selection of Single-Stranded DNA Molecules that Bind and Inhibit Human Thrombin. *Nature* **1992**, *355*, 564–566.
52. Huizenga, D. E.; Szostak, J. W. A DNA Aptamer that Binds Adenosine and ATP. *Biochemistry* **1995**, *34*, 656–665.